Using englacial radar attenuation to better diagnose the subglacial environment: A review

Kenichi Matsuoka *
Department of Earth and Space Sciences
University of Washington
Seattle, WA, USA
matsuoka@ess.washington.edu

Joseph A. MacGregor
Institute of Geophysics
The University of Texas at Austin
Austin, TX, USA
joe.macgregor@gmail.com

Frank Pattyn
Department of Earth sciences and environment
Université Libre de Bruxelles
Brussels, Belgium
fpattyn@ulb.ac.be

***Abstract*— The magnitude of the radar echo returned from beds underneath ice sheets has been used to identify subglacial lakes based on the prediction that wetter and flatter beds have larger reflectivities than dryer and/or rougher beds. Further quantitative diagnosis of the subglacial environment requires accurate correction for englacial dielectric attenuation, which is primarily a function of ice temperature and secondarily a function of ice chemistry. Models show that the attenuation contribution from chemistry (soluble ions) accounts for about one quarter of the attenuation averaged over the full ice thickness at Siple Dome and Vostok in Antarctica. These predictions suggest that a useful initial attenuation estimate across an ice sheet can be obtained simply with ice-temperature modeling. Methods for estimating attenuation from radar data are also reviewed, with an emphasis on the potential pitfalls of individual methods. Some discrepancies exist between attenuation estimated with ice-core data, temperature models, and radar data. We discuss strategies to improve these attenuation estimates.**

Keywords- ice sheets, bed, Antarctica

I. INTRODUCTION

Ice-penetrating radar has been widely used across the Greenland and Antarctic ice sheets to measure ice thickness, image snow/ice stratigraphy, and characterize the subglacial environment [1]. For example, distinct bright and flat reflectors have been interpreted as subglacial lakes [2]. Quantitative analysis of the returned power from the bed can potentially provide a more detailed diagnosis of bed conditions, but this analysis in turn requires a quantitative evaluation of englacial effects upon the radio wave [3]. The two major path effects within the ice overburden are birefringence caused by anisotropic alignments of ice crystals [4, 5], and dielectric attenuation [6]. The effects of birefringence are negligible if appropriate antenna polarizations are used [7]. Therefore, extracting attenuation remains the most significant task in order to quantitatively diagnose bed conditions.

Typical airborne radar studies (e.g. [8] and [9]) have assumed uniform attenuation rates across their study areas and found distinct contrasts in bed reflectivity within the outlets of Kamb and Whillans Ice Streams, West Antarctica. The margins of the higher reflectivity areas roughly match the ice-stream margins, suggesting that bed underneath ice streams is wetter than the bed underneath the inter-ice-stream ridges. However, because attenuation is a function of ice temperature and chemistry [6], attenuation varies spatially. The validity of the assumption of spatially uniform attenuation is therefore uncertain, particularly in areas where the ice-flow regime varies [10].

Here, we review recent studies on englacial attenuation in Antarctic ice sheets and discuss strategies to more quantitatively assess the subglacial environment using ice-penetrating radar.

II. RADAR-ATTENUATION MODELS FOR ICE

Integration of the local attenuation rate from the ice-sheet surface to the bed gives depth-averaged attenuation $\langle N \rangle$. The local one-way attenuation rate N in dB/km is proportional to local ice conductivity σ as:

$$N = \frac{1000\left(10\log_{10} e\right)}{c\varepsilon_0\sqrt{\varepsilon}}\sigma \approx 0.914\sigma\,, \qquad (1)$$

where c is the speed of light in the vacuum and ε_0 is the permittivity of free space. Attenuation rates also depend on the relative permittivity ε, which is a function of ice temperature and chemistry [11]. However, this dependence results in only a ~ ±0.4% difference in N. Depth-variable ε due to densification in the near-surface firn (< ~100 m) has a negligible effect on $\langle N \rangle$ because this depth range is much smaller than the ice thickness (typically ~ 3000 m for inland Antarctica). Here we assume uniform value of ε (= 3.2). Ice conductivity σ is the sum of contributions from pure ice (subscript $i = 0$), acidity ($i =$

* Present address: Norwegian Polar Institute, Tromsø, 9006, Norway.
This research is supported by US NSF grants ANT- 0338151 and ANT-0520541, and in part by the ARC (Action de Recherche Concertée) research project 'IceCube-Dyn' of the Communauté Wallonie-Bruxelles.

978-1-4244-4605-6/09/$25.00 ©2009 IEEE

1), and salinity (i = 2). Individual components have different Arrhenius-type temperature (T) dependence:

$$\sigma = \sum_{i=0}^{2} \sigma_i^0 C_i \exp\left[-\frac{E_i}{k}\left(\frac{1}{T}-\frac{1}{T_r}\right)\right] \quad . \tag{2}$$

where σ^0_i are either pure-ice conductivity (i = 0; μS/m) or molar conductivities (i = 1, 2; μS/m/M, where M = mol/L) at a reference temperature T_r =251 K, C_i (M) are molarities (C_0 = 1, C_1 is acidity, and C_2 is salinity), and E_i are activation energies corresponding to individual components. Ice conductivity linearly depends on the radar-effective acidity and salinity, which depend on the in-situ conditions of the soluble ions [6].

Table I shows mean values and uncertainties for parameters in (2) that have been measured using ice cores and laboratory-grown ice. The pure-ice and acidity parameters are frequency independent across the HF and VHF ranges, while the frequency dependence of these parameters for salinity is not well known. More importantly, most measurements for this compilation were made at temperatures lower than –10°C, so attenuation in warmer ice is not as well constrained at temperatures where the attenuation is largest (Fig. 1).

The molar conductivity for acidity is >7 times larger than that for salinity but their activation energies are similar. Therefore, when the acidity and salinity are equal, the acidity contribution to attenuation at any given temperature is also roughly seven times larger than the salinity. Also, salinity decreases significantly with increasing distance from the coast [12], so the salinity contributions to attenuation are likely less important than acidity and pure-ice contributions for inland Antarctica. Fig. 1 shows the temperature dependence of the pure-ice contribution to local attenuation rate N along with that of the sum of all three components estimated for depth-averaged acidity and salinity measured from ice cores drilled at Siple Dome in West Antarctica (C_1 = 1.3 μM, C_2 = 4.2 μM) and at Vostok in East Antarctica (C_1 = 0.5 μM, C_2 = 2.0 μM).

III. Methods for Estimating Attenuation from Radar Data

There are currently five methods to estimate attenuation from radar data. Four of these methods estimate the depth-averaged attenuation rate $\langle N \rangle$ from the relationship between bed-returned power P_{bed} and the englacial path length $2L$. The fifth method uses depth variations of the radar power returned from within the ice.

TABLE I. Conductivity Parameters in (2)

Symbol	Description	Value [a]
σ^0_0	Conductivity of pure ice	7.2 ± 3.1 (9.2 ± 0.2) μS/m
σ^0_1	Molar conductivity of acidity	3.2 ± 0.5 S/m/M
σ^0_2	Molar conductivity of salinity	0.43 ± 0.07 S/m/M
E_0	Activation energy of pure ice	0.55 ± 0.05 (0.51 ± 0.01) eV
E_1	Activation energy of acidity	0.20 ± 0.04 eV
E_2	Activation energy of salinity	0.19 ± 0.02 eV
T_r	Reference temperature	251 K

a. Mean and uncertainty of values summarized by [6]. Values for pure ice shown in the parentheses are from [14], which produce a better match between ice-core-based and radar-based estimates of the attenuation at Siple Dome, and used to derive the pure-ice contribution in this paper.

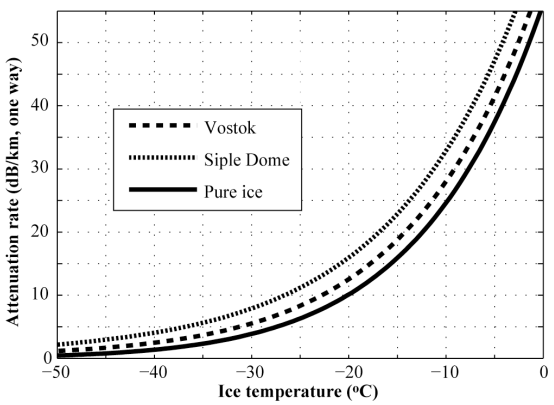

Figure 1. Temperature dependence of the attenuation contributions from pure ice, and ice including soluble ions at levels of depth-averaged acidity and salinity at Siple Dome in West Antarctica and Vostok in East Antarctica.

The radar power returned from the bed can be written in the decibel scale as [13]:

$$[P_{bed}]_{dB} = [S]_{dB} - [G_{bed}]_{dB} + [R_{bed}]_{dB} - 2\langle N \rangle L. \tag{3}$$

Where S represents instrumental factors including the transmitted power and system gain, G_{bed} is the loss due to geometric spreading, and R_{bed} is bed reflectivity. G_{bed} can be derived from height h of the radar above the surface and one-way path length in the ice as $G_{bed} = \left(h + L/\sqrt{\varepsilon}\right)^2$. If the surveyed region contains surface, buried, and/or basal crevasses, the scattering loss may be significant and should also be included in (3). For radar-profiling data across Siple Dome, [15] used the relationship between P_{bed} and L to empirically remove the contributions from terms other than R_{bed}. They found that R_{bed} remains nearly unchanged across the profile. Similar analyses were made for relict ice streams near Siple Dome [16] and the crevassed lateral (shear) margins of Whillans and Kamb Ice Streams [17]. These studies revealed significant variations in the bed reflectivity that are correlated with changing ice-flow regimes. However, none of these studies directly calculated $\langle N \rangle$ from their radar data.

When the ice sheet is stratified and crevasse-free, neither englacial scattering nor loss caused by multiple reflections between ice layers are significant [6], so (3) is valid. For a unit change of path length δL, variations in the geometrically-corrected returned power $[P^c_{bed}]_{dB}$ (=$[P_{bed}]_{dB}$ + $[G_{bed}]_{dB}$) from the bed are

$$\delta[P^c_{bed}]_{dB} = \delta[S]_{dB} + \delta[R_{bed}]_{dB} - 2\langle N \rangle \delta L. \tag{4}$$

$\langle N \rangle$ can be calculated from $\delta[P^c_{bed}]_{dB}/\delta L$, if S and R_{bed} remain unchanged. In this way, attenuation was estimated using radar-profiling data from Siple Dome [6, 18] and in Kamb Ice Stream [19]. We emphasize that it is critical to examine stability of S and, most importantly, the uniformity of R_{bed} for this analysis. All else being equal, thicker ice better insulates the bed from

the downward vertical advection of cold ice, so the bed underneath thicker ice is more likely to be thawed and have a larger reflectivity than the bed underneath thinner ice. This relationship infers that R_{bed} is inherently spatially correlated with ice thickness, which may result in erroneously smaller estimates of $\langle N \rangle$.

When both single- and double-bounced bed echoes are observed, attenuation can be estimated using the ratio of the returned power of these two echoes [10]. The double-bounced echoes have been observed over thin ice shelves. An advantage of this method is that the instrumental factor is effectively identical for both of these echoes, so $\delta[S]_{dB}$ is negligible.

Reference [18] developed a method for estimating attenuation using common-midpoint (CMP) radar data. In CMP measurements, the path length varies as a function of the ice thickness and the distance between radar transmitter and receiver. The incident angle dependence of the Fresnel reflectivity of the bed is independent of the magnitude of the dielectric contrast at the bed (i.e. wetness of the bed). Thus, if the bed is smooth enough relative to the radar wavelength, $\delta[R_{bed}]_{dB}$ can be modeled with the angular dependence of the Fresnel reflectivity. The antenna-beam pattern should also be accounted for within $\delta[S]_{dB}$. This method can therefore determine attenuation independent of the bed condition. The use of low frequencies (HF or low VHF) is also necessary with this method to avoid effects of birefringence [5].

The above methods all rely upon varying path lengths to vary the bed-returned power and derive $\langle N \rangle$. The uncertainty in the returned power is typically up to several decibels, inferring that L should be changed more than the e-folding length L_0 (= $1000(10\log_{10}e)/\langle N \rangle$), where L_0 is in units of meters. Table II shows that $\langle N \rangle$ ranges between ~9 and ~35 dB/km in Antarctica, which corresponds to L_0 between ~482 m and ~120 m. For CMP measurements on 3-km-thick ice, the separation between the transmitter and receiver should be changed to ~1.2 km (L_0 = 120 m) and ~2.4 km (L_0 = 482 m), which is currently challenging due to technical issues.

The fifth method uses the returned power from within the ice, not from the bed [13]. At a given location, depth (vertical) variations of the englacial returned power are related to depth variations of the englacial reflectivity and attenuation. The dominant cause of reflections at low frequencies (< ~100 MHz) is acidity contrasts at depths ~500 m or more below the surface [20]. At these frequencies, englacial reflectivity is therefore a function of acidity contrasts and ice temperature. This assumption simplifies the interpretation of depth variations of the returned power in isothermal ice. If ice chemistry varies minimally along the propagation path [6], then the attenuation rate is uniform and thus returned power is expected to decrease linearly in the isothermal ice. Based on this prediction, vertical gradients of the returned power were derived every ~12 m along radar profiles using 60-MHz airborne radar data collected in central West Antarctica (WAIS Divide) where isothermal ice is predicted in the upper half or more [13, 21]. Derivation of attenuation using this method was confounded by anomalously small reflectivities of tilted internal layers above steep beds. To mitigate this effect, data ensembles are made using radar data collected over a distance much wider than the anomalous features in the returned power. The depth profiles of these ensembles show a clear upper cutoff of the returned power from a given depth and that this cutoff decreases linearly, constituting the upper envelope of the returned power. The vertical gradient of this envelope can represent the englacial attenuation rate averaged over that isothermal ice [13]. This method can be applied in other areas including southern Greenland, where accumulation is large relative to ice thickness so that thick isothermal ice is expected.

TABLE II. ESTIMATED ATTENUATION

Site	Attenuation (dB/km, one way) [a]		
	Radar	Ice core [b]	Temperature -model [c]
Vostok	--	8.9 [7.0][d1]	5.1
Siple Dome	35[d2A] 25.3[d3B]	24 [7.8][d3]	15.7
Kamb Ice Stream	14.9[d4B] 19.8[d4B]	--	~25
WAIS Divide	10.4[d5C]	--	~2

a. These are averaged over the entire ice column to the bed, but the value at WAIS Divide is a mean from the surface to roughly half of the ice thickness (~1800 m).

b. Values in the brackets account only for the pure-ice contribution (2) using dielectric parameters from [14], shown in parentheses in Table I.

c. The pure-ice contributions are accounted for this estimate using dielectric parameters from [14].

d. Data sources are 1: [22], 2: [18], 3: [6], 4: [19], 5: [13]. Radar methods to derive attenuation are A: CMP, B: lateral variation of ice thickness, C: depth variations of englacial returned power.

IV. ATTENUATION ESTIMATES

Table II summarizes radar-measured attenuation rates at various sites in Antarctica. Additional measurements exist, but they either assumed a value of the bed reflectivity to estimate attenuation from the bed returned power [23, 24], or that only the difference in attenuation between two sites is known [25]. Table II also shows depth-averaged attenuation rates modeled using (1), (2), and measured ice chemistry and temperature at Siple Dome (ice thickness: 1004 m) and at Vostok (3755 m). Half of the attenuation occurs within the deepest 30% and 12% of the ice thickness at Siple Dome and Vostok, respectively, because the depth profile of attenuation rate is dominated by its temperature dependence (Fig. 1) and the temperature varies rapidly near the beds. Depth profiles of the local attenuation rate N (2) have many spikes mostly associated with volcanic eruptions, but which have a negligible effect upon the depth-averaged attenuation rate because such peaks are localized within narrow depth ranges [6]. This suggests that attenuation modeling requires only relatively low-resolution depth profiles of chemistry. The pure-ice contribution accounts for 74% and 79% of the total attenuation at Siple Dome and Vostok, respectively, so it should therefore be possible to roughly estimate attenuation over the entire ice sheet using information regarding ice temperatures only.

We estimated the pure-ice contribution to the attenuation using (2), dielectric parameters for [14] (Table I), and ice temperature derived with a continental-scale three-dimensional ice-flow model [26]. In this steady-state model, ice temperature is coupled with ice flow that is balanced by the

modern surface accumulation, thereby matching the current surface topography. Ice temperature is estimated on a 5-km horizontal grid across Antarctica with 21 vertical layers whose separation decreases closer to the bed. Boundary conditions (geothermal flux and surface accumulation) are tuned using depth profiles of ice temperature measured at 9 boreholes. Geothermal flux is further tuned so that the bed temperature at known subglacial lakes reaches the pressure melting point. As a result, the predicted ice temperature at boreholes does not perfectly match the observed one especially at great depths. Tuning with subglacial lakes is useful since there are only 9 boreholes but more than 270 subglacial lakes. Overall, modeled ice temperatures at 9 boreholes are predicted very close to the observed profiles, but an exponential relationship between ice temperature and attenuation (2) yields temperature-modeling-based attenuation rates that are ~ 2dB/km larger than the borehole-temperature-based predictions at Siple Dome and Vostok (Table II).

V. Discussion and Outlook

We used the expected contrast of the Fresnel reflectivity of wet and dry beds (10–15 dB [9]) to inform the necessary accuracy in the attenuation estimate. When bed reflectivity and depth-averaged attenuation vary $\delta[R_{bed}]_{dB}$ and $\delta\langle N\rangle L$ over a uniform ice thickness ($L/2$), the returned bed power varies by $\delta[R_{bed}]_{dB} - \delta\langle N\rangle L$. Assuming $\delta[R_{bed}]_{dB}$ = 15 dB and $L/2$ = 3 km, the apparent returned bed power from wet and dry beds is effectively identical if $\langle N\rangle$ for the dry bed is 2.5 dB/km larger than that for the wet bed. The spatial variability of attenuation in the upper half of the ice sheet measured in central West Antarctica is ~ 5 dB/km (one way), which causes an 18 dB difference in attenuation within the upper half of the ice sheet (~ 1800 m) [13]. This result suggests that accurate derivation of bed reflectivity certainly requires consideration of the spatial variability of attenuation.

None of the methods described in Section III are yet adequate to estimate the depth-averaged attenuation rate at the necessary level of accuracy. Analysis of the englacial returned power can provide the englacial attenuation independent of bed reflectivity, but this method is applicable only within the upper part of the ice sheet. The other profiling methods can resolve the depth-averaged attenuation rate through the entire ice column but rely on the assumption that bed reflectivity varies independently of the ice thickness. The CMP method is time consuming and thus has significant potential only for point estimates.

The pure-ice contribution is the most significant contribution to the attenuation in most cases. However, individual measurements of σ^0_0 show large (43%) variability (Table I). This variation results in an attenuation-rate difference of ~17 and ~7 dB/km at temperatures of –10 and –20°C, respectively. Measurements of σ^0_0, especially at temperatures close to the pressure melting point, should therefore be of the highest priority to ensure more accurate modeling of attenuation. Relative to uncertainties in the pure-ice parameters for the attenuation model (Table I), the mismatches between modeled and measured ice temperatures are small.

The acidity and salinity contributions still account for a quarter of the attenuation, so that it is important to model the spatial variability of ice chemistry and include that variability in attenuation modeling. Attenuation estimated in the upper half of central West Antarctica is significantly higher than that predicted solely using the pure-ice contribution (Table II). In central Antarctica, the observed variations in attenuation suggest that acidity could vary by up to a factor of two within a ~120 km by ~120 km area [13]. These results suggest that the acidity and salinity components can also be important for estimating the regional variation of attenuation.

The geometry of radar layers has been interpreted in terms of ice-sheet evolution using ice-flow models [27], but most models assume a uniformly dry bed. Even if the same radar data are used to derive both returned power and geometry of layers, these properties are independent of each other in terms of their measurement. Modeled ice temperature can be used to calibrate the bed returned power, which, in turn, could be used to constrain the spatial variability of the bed conditions. Self-consistent iterations between these steps will result in the best possible predictions of the current bed conditions and evolution of the ice sheet. Finally, estimated attenuation may also be used to constrain the chemical structures of the ice, which can significantly affect ice rheology [28].

Acknowledgment

This paper was stimulated by discussions with Dale P. Winebrenner, Edwin D. Waddington, Howard Conway and Charles F. Raymond from University of Washington.

References

[1] Bogorodskiy, V.V., Bentley, C.R., and Gudmandseon, P., Radioglaciology, D. Reidel, 1985.

[2] Siegert, M.J., Carter, S., Tabacco, I., Popov, S., and Blankenship, D.D., "A revised inventory of Antarctic subglacial lakes", Antarctic Science, 17, (3), pp. 453-460, 2005.

[3] Carter, S.P. et al.: "Radar-based subglacial lake classification in Antarctica", Geochem. Geophys. Geosys., doi: 10.1029/2006gc001408, 2007.

[4] Fujita, S., Maeno, H., and Matsuoka, K., "Radio-wave depolarization and scattering within ice sheets: a matrix-based model to link radar and ice-core measurements and its application", J. Glaciol., 52, (178), pp. 407-424, 2006.

[5] Matsuoka, K., Wilen, L., Hurley, S.P., and Raymond, C.F., "Effects of Birefringence Within Ice Sheets on Obliquely Propagating Radio Waves", IEEE Trans. Geosci. Rem. Sens., 47, (5), pp. 1429-1443, 2009.

[6] MacGregor, J.A. et al., "Modeling englacial radar attenuation at Siple Dome, West Antarctica, using ice chemistry and temperature data", J. Geophys. Res., 112, (F3), pp. doi:10.1029/2006JF000717, 2007.

[7] Matsuoka, K. et al., "Crystal orientation fabrics within the Antarctic ice sheet revealed by a multipolarization plane and dual-frequency radar survey", J. Geophys. Res., 108, (B10), doi:10.1029/2003JB002425, 2003.

[8] Bentley, C.R., Lord, N., and Liu, C., "Radar reflections reveal a wet bed beneath stagnant Ice Stream C and a frozen bed beneath ridge BC, West Antarctica", J. Glaciol., 44, (146), pp. 149-156, 1998.

[9] Peters, M.E., Blankenship, D.D., and Morse, D.L., "Analysis techniques for coherent airborne radar sounding: Application to West Antarctic ice streams", J. Geophys. Res., 110, (B6), doi:10.1029/2004JB003222, 2005.

[10] MacGregor, J.A., Anandakrishnan, S., Winebrenner, D.P., Catania, G., and Joughin, I., "Multiple bed echoes, englacial radar attenuation, and basal reflectivity across the grounding line of the Siple Coast, West Antarctica", J. Geophys. Res., submitted.

[11] Fujita, S., Matsuoka, T., Ishida, T., Matsuoka, K., and Mae, S., "A summary of the complex dielectric permittivity of ice in the megahertz range and its applications for radar sounding of polar ice sheets", in Hondoh, T. (Ed.): 'Physics of Ice Core Records' (Hokkaido University Press, 2000), pp. 185-212.

[12] Suzuki, T. et al., "Distribution of sea salt components in snow cover along the traverse route from the coast to Dome Fuji station 1000 km inland at east Dronning Maud Land, Antarctica", Tellus Series B, 54, (4), pp. 407-411, 2002.

[13] Matsuoka, K., Morse, D., and Raymond, C.A., "Estimating englacial radar attenuation using depth profiles of the returned power, central West Antarctica", J. Geophys. Res., in press.

[14] Johari, G., and Charette, P., "The permittivity and attenuation in polycrystalline and single-crystal ice Ih at 35 and 60 MHz", J. Glaciol., 14, pp. 293-303, 1975.

[15] Gades, A.M., Raymond, C.F., Conway, H., and Jacobel, R.W., "Bed properties of Siple Dome and adjacent ice streams, West Antarctica, inferred from radio-echo sounding measurements", J. Glaciol., 46, (152), pp. 88-94, 2000.

[16] Catania, G.A., Conway, H.B., Gades, A.M., Raymond, C.F., and Engelhardt, H., "Bed reflectivity beneath inactive ice streams in West Antarctica", Ann. Glaciol., 36, pp. 287-291, 2003.

[17] Raymond, C.F., Catania, G.A., Nereson, N., and Van der Veen, C.J., "Bed radar reflectivity across the north margin of Whillans Ice Stream, West Antarctica, and implications for margin processes", J. Glaciol., 52, (176), pp. 3-10, 2006.

[18] Winebrenner, D.P., Smith, B.E., Catania, G.A., Conway, H.B., and Raymond, C.F., "Radio-frequency attenuation beneath Siple Dome, West Antarctica, from wide-angle and profiling radar observations", Ann. Glaciol., 37, pp. 226-232, 2003.

[19] Jacobel, R., Welch, B.C., Osterhouse, D., Pettersson, R., and MacGregor, J.A., "Spatial variation of radar-derived basal conditions on Kamb Ice Stream, West Antarctica", Ann. Glaciol., 50, (51), pp. 10-16, 2009.

[20] Fujita, S. et al., "Nature of radio echo layering in the Antarctic ice sheet detected by a two-frequency experiment", J. Geophys. Res., 104, (B6), pp. 13013-13024, 1999.

[21] Morse, D.L., Blankenship, D.D., Waddington, E.D., and Neumann, T.A., "A site for deep ice coring in West Antarctica: results from aerogeophysical surveys and thermo-kinematic modeling", Ann. Glaciol., 35, pp. 36-44, 2002.

[22] MacGregor, J.A., Matsuoka, K., and Studinger, M., "Radar detection of accreted ice over 1 Lake Vostok, Antarctica", Earth Planet. Sci. Lett., 282, pp. 222-233, 2009.

[23] Barwick, S., Besson, D., Gorham, P., and Saltzberg, D., "South Polar in situ radio-frequency ice attenuation", J. Glaciol., 51, (173), pp. 231-238, 2005.

[24] Besson, D.Z. et al., "In situ radioglaciological measurements near Taylor Dome, Antarctica and implications for ultra-high energy (UHE) neutrino astronomy", Astroparticle Phys., 29, (2), pp. 130-157, 2008.

[25] Corr, H., Moore, J.C., and Nicholls, K.W., "Radar Absorption Due to Impurities in Antarctic Ice", Geophys. Res. Lett., 20, (11), pp. 1071-1074, 1993.

[26] Pattyn, F., "Antarctic subglacial conditions inferred from a hybrid ice sheet/ice stream model", Earth Planet. Sci. Lett., submitted.

[27] Waddington, E.D., Neumann, T.A., Koutnik, M.R., Marshall, H.P., and Morse, D.L., "Inference of accumulation-rate patterns from deep layers in glaciers and ice sheets", J. Glaciol., 53, (183), pp. 694-712, 2007.

[28] Thorsteinsson, T., Waddington, E.D., Taylor, K.C., Alley, R.B., and Blankenship, D.D., "Strain-rate enhancement at Dye 3, Greenland", J. Glaciol., 45, (150), pp. 338-345, 1999.